

HETEROCYCLES, Vol. 105, No. 1, 2022, pp. 461 - 476. © 2022 The Japan Institute of Heterocyclic Chemistry  
Received, 27th February, 2022, Accepted, 11th April, 2022, Published online, 25th April, 2022  
DOI: 10.3987/COM-22-S(R)17

## 2-ARYLAZOIMIDAZOLES REVAMPED BY QUARTERNIZATION OR DIMERIZATION; ANOTHER GAIN IN FUNCTIONALITY OF AN INDUSTRIAL DYESTUFF FAMILY BY TASK-SPECIFIC SIDE-CHAIN SUBSTITUENTS

Sandro Neuner,<sup>1</sup> Heidi A. Schwartz,<sup>1</sup> Christoph Kreutz,<sup>2</sup> Thomas Müller,<sup>2</sup> Paul Mayer,<sup>3</sup> Günther Bonn,<sup>3</sup> Thomas Gelbrich,<sup>4</sup> Ulrich J. Griesser,<sup>4</sup> Klaus Wurst,<sup>1</sup> Volker Kahlenberg,<sup>5</sup> Sven Nerdinger,<sup>6\*</sup> and Herwig Schottenberger<sup>1\*</sup>

<sup>1-5</sup>Leopold Franzens University, 6020 Innsbruck, Austria; <sup>1</sup>Institute of General, Theoretical & Inorganic Chemistry, Innrain 80-82; <sup>2</sup>Institute of Organic Chemistry, Innrain 80-82; <sup>3</sup>Institute of Analytical Chemistry, Innrain 80-82; <sup>4</sup>Institute of Pharmacy, Innrain 52c; <sup>5</sup>Institute of Mineralogy & Petrography, Innrain 52; <sup>6</sup>Sandoz GmbH, Biochemiestr. 10, 6250 Kundl, Austria. E-mail: sven.nerdinger@sandoz.com; Herwig.Schottenberger@uibk.ac.at.

This paper is dedicated to Professor Somsak Ruchirawat on the occasion of his 80th birthday.

**Abstract** – Based on [(*E*)-2-(4-fluorophenyl)diazenyl]-1*H*-imidazole, [210180-24-0], a versatile late stage intermediate for the divergent synthesis of direct dyes, a novel series of *N,N'*-disubstituted azoimidazolium salts was prepared. In particular, benzylation, 4-vinylbenzylation, phenacylation, sulfopropylation, ethylation, as well as propargylation allowed for the access of derivatives (**1-6**), which are useful for follow-up conversions, *e.g.* click reactions, or free radical polymerization. The compounds were routinely characterized spectroscopically. The diethylated tetrafluoroborate salt **5** was additionally analyzed by <sup>19</sup>F-NMR. Hot stage microscopy of contact melts of **5** with the less commonly used anionic nucleophiles azide and rhodanide illustrate the rapid formation of deeply colored products confirming the nucleophilic aromatic replacement of fluoride in the 4-fluorophenyl substituent. Remarkably, in addition to the conceived functional quarternizations, a neutral dimer chromophore (**7**) resulted from using

epichlorohydrin as a linking agent. Single crystal X-ray structure determinations are reported for all newly described compounds.

## INTRODUCTION

2-(Arylazo)imidazoles have long been described in literature. Their first representatives can truly be considered chemical fossils. For example, the renowned biochemical Pauly's test for the detection of histidine (and tyrosine) contained in protein samples, where diazotized sulfanilic acid couples with imidazole, is dated back to around the year 1904.<sup>1</sup> Shortly thereafter, targeted investigations showed that the coupling occurs at the C2-position of the *N*-unsubstituted imidazoles.<sup>2</sup> Mechanistic studies revealed, that in the case of azo couplings onto imidazole, the corresponding anion is involved. Otherwise, with *N*-substituted or neutral imidazoles, it was evidenced, that reversible attacks of aryldiazonium reactants occur on a ring nitrogen.<sup>3</sup> Thus, certain conditions must be met for uniform coupling, since isomeric coupling products, as well as bis- and trisazo-compounds, can also be formed. The tendency to such side reactions is also influenced by the type of diazo compound used as well as by the substitution of the imidazole (see also synthetic considerations section).<sup>4</sup>

Nevertheless, technical and scientific improvements have been made continuously since then. At present, light-switchable azoimidazoles enrich research regarding photoisomerisation,<sup>5</sup> photochromism of liquid crystals,<sup>6</sup> redox-responsive metal chelating agents,<sup>7</sup> and general coordination chemistry,<sup>8</sup> and, last but not least, photodissociable ligands of highly sophisticated spin state-switchable nickel porphyrins.<sup>9</sup>

But an even more fascinating area of azole-based azo-dye chemistry has been tapped by researchers from leading German corporate industry, when they started to explore the reactive behavior of quarternized 2-arylazoimidazolium salts containing halogenated phenyl moieties. In their pioneering work, chemists from BASF, as headed (and excellently reviewed) by Baumann and Dehnert,<sup>4</sup> it was first established that quaternary salts of 2-(4-chlorophenylazo)imidazole react very readily with amines, exchanging the chlorine atom for the amine residues and usually yielding red dyes. The reaction works particularly well with secondary aliphatic amines. In addition, it was found that weaker basic amines, especially those of the realm of aromatic ones, require more vigorous reaction conditions, or tertiary amines as catalysts.

Thus, a huge variety of dyes of this series could be made accessible from numerous and easily available starting products in a gentle reaction. Such efforts must be systematically performed with respect to coloristic requirements for shade, fastness properties and fibre dyeing behavior.

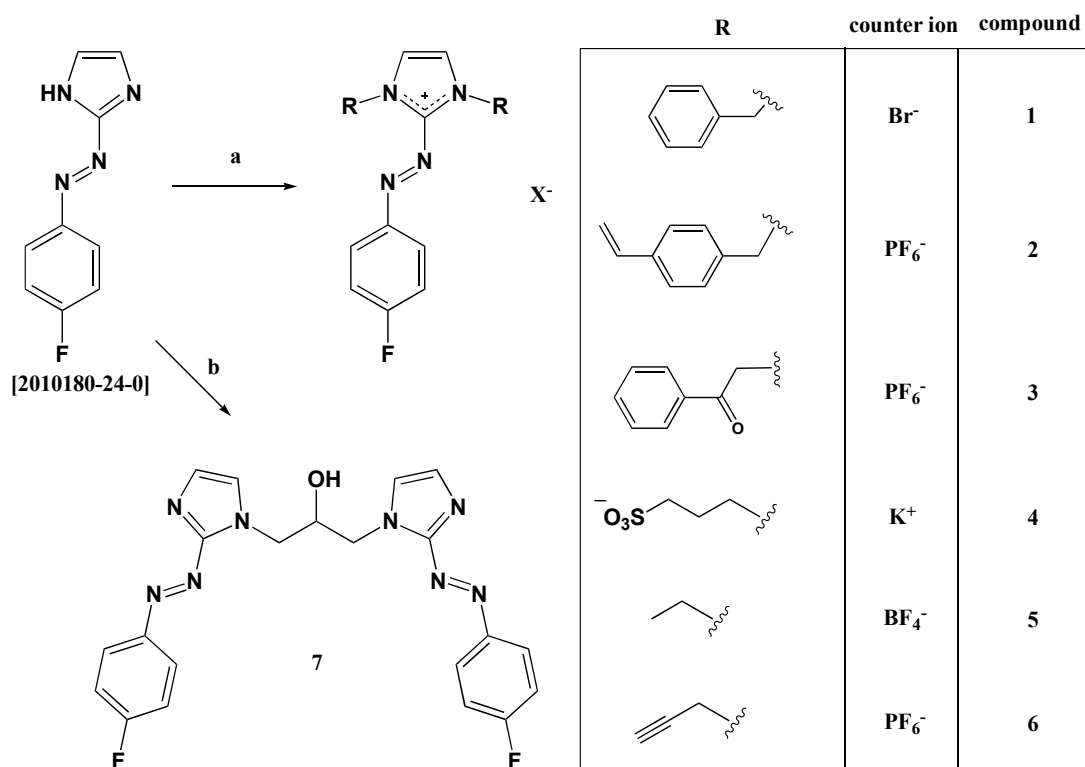
Furthermore, this  $S_NAr$  amination was found to be not limited to the substitution of halogen atoms. It can generally be carried out with anionically cleavable substituents such as hydroxyl, alkoxy, sulfonic acid or sulfonic acid ester groups. Remarkably, the exchange of a fluorine atom for nucleophiles proceeds at a much higher rate than that of the chlorine atom, which was presumed to be another indication of the

classical stepwise addition mechanism of this  $S_NAr$  displacement involving a carbenium structure.<sup>10</sup> Even those quaternary salts in which the aromatic nucleus is directly linked to the heterocycle could not be converted with amines. The azo group, in addition to the heterocycle, is thus one of the determining factors for the electrophilic character of this family of quaternary salts. Amazingly, this azo-group effect can also be underlined by the finding that, under somewhat harsher reaction conditions, even the neutral 4-fluorophenylazoimidazole [210180-24-0] can undergo nucleophilic aromatic fluoride replacement.<sup>11</sup> Subsequently, the inspiring and fundamental work of the BASF-group resulted in a large number of patent applications, mainly related to thiolated direct dyes<sup>12</sup> or disulfide protected formulations<sup>13</sup> for staining keratin or polyamide fibers, besides the well-established zinc chloride double salt dyes.<sup>14</sup> Moreover, the 2-arylaazoimidazolium head group, flanked with elongated alkyl chains was introduced to design chromophoric surfactants with dual photo/redox responsiveness.<sup>15</sup>

## RESULTS AND DISCUSSION

### SYNTHETIC CONSIDERATIONS

In the present contribution our aim was to build up a tentative platform of refurbished arylazoimidazoles (Scheme 1), which should be featured atypically by task specific substitution patterns.



**Scheme 1.** Synthetic overview of task-specifically functionalized 4-F-phenylazoimidazoles. Conditions: a) 1-1.2 eq. base, 2.2-5 eq. electrophile, 0 °C - reflux, b) 1.1 eq. KOEt, 0.6 eq. epichlorohydrin, rt

In conclusion, their inestimable scope of applications may not only be further developed by the concepts outlined herein, in particular hydrazine chemistry, acetylenic or vinylic coupling and polymerization routes (which are self-evidently covered by compounds **3**, **6**, and **2**, respectively), but, eventually, by the aforementioned  $S_NAR$  derivations,<sup>4</sup> since the subsequent functionalization at the halogenated sites of haloarylazoimidazolium salts represents a synthetic permutation toolkit in its own right<sup>4</sup> (see also thermoanalytical part and supporting information for **5**).

As already referenced,<sup>3,4</sup> the clean coupling of imidazolate with aryldiazonium is requiring careful reaction conditions, in particular control of pH and of course reaction temperature. The involvement of the imidazole anion was explained on kinetic evidence, pressure studies, and MNDO calculations.<sup>3</sup> *N*-Methylation was shown to affect not only the kinetics of the reaction but also the products.<sup>3</sup> With the neutral form of imidazole it was suspected that triazene formation is the predominant pathway. Anyway, the final removal of the imidazole C2-proton is still lacking mechanistic clarification. For example, own experiments<sup>16</sup> showed that deprotonation of 1-vinylimidazole using strong bases, such as isopropylmagnesium chloride proceeds satisfactorily (with subsequent addition of elemental sulfur yielding 1-vinyl-4-imidazoline-2-thione, hereby confirming the desired attack at the C2-position). Upon addition of isolated arenediazonium tetrafluoroborates to 1-vinylimidazole solutions in THF, the reaction mixture immediately undergoes a red coloration, but, disappointingly, no *N*-vinylated phenylazoimidazole system could be straightforwardly isolated so far.

Therefore, the approach to prepare presubstituted neutral arylazoimidazoles via direct charge annihilating ion collisions of diazonium with monosubstituted imidazoles does not seem to represent an attractive general strategy despite the hereby possible derivatives bearing different *N*-substituents after quarternization would be of high demand.

Alternatively, but at the price of greater effort in terms of access to starting materials, free nitrogen heterocyclic carbenes (NHC carbenes), evidently with the sidechains already incorporated, are capable of adding diazonium ions directly to yield arylazoazolium salts.<sup>17</sup>

For the 1,3-diarylimidazolium family, such representatives exhibit very high stability and light fastness in addition to brilliant hue.<sup>18</sup>

With at least the classical<sup>4</sup> unsubstituted arylazoimidazoles at hand, the new quarternization variants proceeded as expected with ease (see scheme 1). However, the somewhat exceptional bifunctional electrophile epichlorohydrin, which is widely used in azole quarternizations, behaved differently in our case than previously described in the literature.<sup>19</sup>

Under appropriate conditions, partial bridging yielded 1,3-bis(2-(4-fluorophenyl)diazenyl)-1*H*-imidazol-1-yl)propan-2-ol (**7**) instead of quarternization. After rational double quarternization, this dimer chromophore represents a valuable supplementation to methylene linked azoimidazole systems<sup>20</sup> and may

serve as an interesting crosslinker. For example, polyelectrolytes consisting of such bis(arylaazoimidazolium) salts attached by  $S_NAr$  onto polyethylene imine,<sup>21</sup> could be realized even as polymer-crosslinked variants.

## THERMAL ANALYSIS

To investigate the reaction of compound **5** with the rather strong nucleophiles azide ( $Bu_4N^+N_3^-$ ) and thiocyanate (KSCN) under solvent free conditions, hot stage microscopy and thermogravimetric analysis (TGA) were applied. Polarized light hot stage microscopy is a reliable method to visualize optical changes of crystalline materials caused by phase changes or chemical reactions under precise temperature control and thermogravimetry allows to quantify the amount of volatile reaction products. Figures 1a and 1b show polarized light photomicrographs of the contact zone (for further experimental details see supporting info) of a recrystallized melt film of **5** with the liquid of  $Bu_4N^+N_3^-$  at 70 and 80 °C respectively. The reaction starts around 70 °C and accelerates with increasing temperature indicated by the formation of nitrogen bubbles and the formation of a deep red dye which dissolves in the melt of  $Bu_4N^+N_3^-$ . The contact preparation of **5** with KSCN (Figure 1c) also results in a deep purple colored liquid besides a non-birefringent solid phase, which precipitates quickly in the reaction zone. The contact preparation requires a temperature of 175 °C (melting point of KSCN) where the reaction rate is very fast.



**Figure 1.** Polarized light photomicrographs of the recrystallized melt of the yellowish colored, dichroic 2-(4-fluorophenyl)diazenyl)-1,3-diethylimidazolium tetrafluoroborate (**5**) in contact with the undercooled melt of (a, b) tetrabutylammonium azide (Mp 89 °C) and the melt of (c) KSCN (Mp 175 °C). a) image recorded at 70 °C (start of the reaction); b) at 80 °C showing the fast production of nitrogen bubbles under formation of a deep purple secondary dye diffusing into liquid  $Bu_4N^+N_3^-$ ; c) contact zone after melting KSCN at 175 °C resulting in a deep purple dye and a greyish precipitate (supposedly  $KBF_4$ ).

Figure 2 displays the results of the thermogravimetric analysis of a mixture of one molar equivalent of **5** with two equivalents of  $Bu_4N^+N_3^-$  along with the thermograms of the pure reactants. The mixture shows a

sharp step with 3% mass loss between 70 and 80 °C indicating the release of N<sub>2</sub>, consistent with the thermomicroscopic observations. This behavior suggests the consumption of one mole of N<sub>3</sub><sup>-</sup>, followed by the elimination of one molecule of N<sub>2</sub>, supposedly forming an intermediate nitrene, which then most likely undergoes insertions, dimerization and other unidentified degradative quenching. Notably, a related 2-azidoimidazolium parent system without the 4-phenyleneazo interlink was reported to be quite unstable at room temperature in the presence of excess azide, thus causing a total liberation of three equivalents of N<sub>2</sub>, which would result in the formation of carbene intermediates.<sup>22</sup>

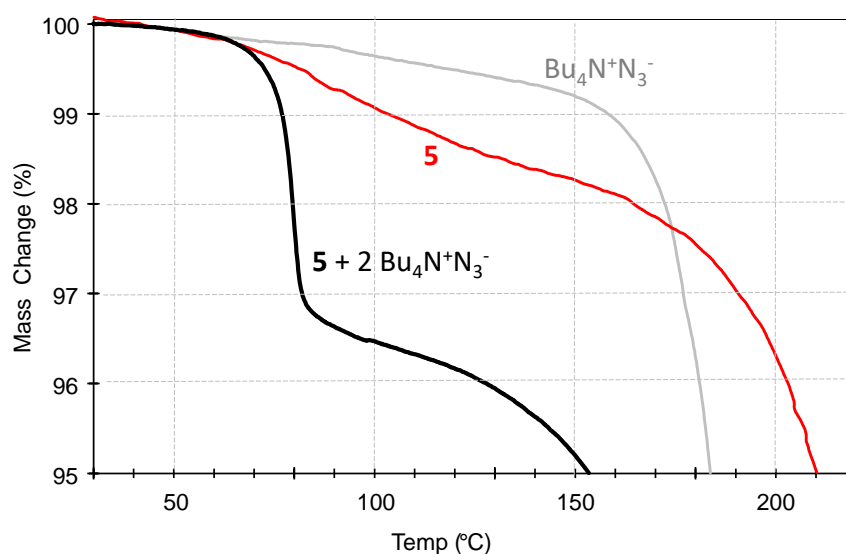


**Figure 2.** Thermogravimetric recording of compound **5**, tetrabutylammonium azide and a 1:2 mixture of the two compounds (heating rate 2 K min<sup>-1</sup>)

## CRYSTAL STRUCTURES

The crystallographic data for the structure determinations are collected in Table 1. The asymmetric unit of **1** (Figure 3) contains one formula unit. The cation shows the expected bond geometries with an almost planar ((4-fluorophenyl)diazenyl)-1*H*-imidazolium (FPDI) unit. The two benzyl substituents of the imidazolium are *cis* and the mean planes of their aromatic rings form an angle of 56.3°.

Compound **2** forms a crystal structure containing one half of a 4-vinylbenzyl chloride (4-VBnCl) molecule per formula unit as an additional component (*i.e.* **2** · **0.5 4-VBnCl**; Figure 3). The FPDI unit of the cation is almost perfectly planar, and the vinylbenzyl substituents are found in a *cis* conformation. The mean planes of their aromatic rings form an angle of 20.7°. The disordered 4-VBnCl molecule is located in a special position on an inversion centre and exists as four distinct disorder fragments having relative occupancies of 30%, 30%, 20% and 20% (Figure S1 of the Supporting Information), where the first and second components differ only in that the –CH<sub>2</sub>–Cl and –CH=CH<sub>2</sub> ring substituents swap their positions. The same relationship also applies for the third and fourth disorder component.

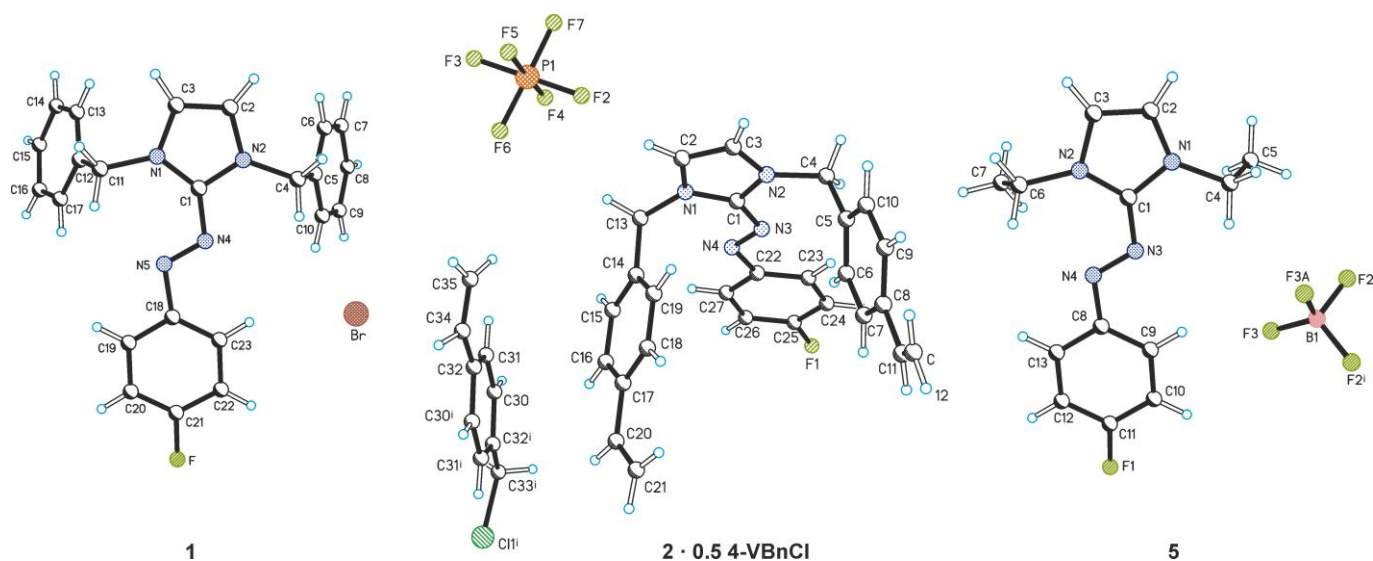


**Figure 3.** Molecular structures of **1**, **2 · 0.5 4-VBnCl** and **5**

The asymmetric unit of compound **3** contains one formula unit (Figure 4). The planarity of the central FPDI fragment of the cation is severely disturbed, resulting in a  $40.4^\circ$  angle between the mean planes of its imidazolium and phenyl rings. The phenyl ring of FPDI is situated in relatively close proximity to the centre (Cg) of the aromatic ring of the 2-oxo-2-phenylethyl unit, resulting in a short separation of C25–H...Cg 2.93 Å. The unusual twist of the FPDI unit is caused by steric effects and prevents an even closer (repulsive) intermolecular contact. The arrangement of the two substituents of the imidazolium ring is *cis*. In the anion, the set of six F atoms is disordered over two positions (occupancy ratio 57:43).

The structure of compound **4** contains two crystallographically independent formula units (Figure 4). The FPDI is close to planar, and the ring substituents propane-1-sulfonate are *cis*. Each of the two potassium centres, K1 and K2, is coordinated by seven sulfonate-O atoms belonging to five different sulfonate groups (Figure S2 of the Supporting Information). The corresponding K1–O coordination distances lie between 2.711(8) and 2.869(8) Å, and the K1–O distances range from 2.666(6) to 3.024(14) Å. Neighbouring KO<sub>7</sub> polyhedra are edge-connected (K1/K1, K2/K2) or face-connected (K1/K2) and form infinite chains which propagate parallel to the *a* axis. Altogether, a three-dimensional coordination framework is formed, which contains large open channels along the [100] direction, offering 125 Å<sup>3</sup> of solvent-accessible void space per formula unit (see Figure S3 of the Supporting Information). It was not possible to obtain a viable model for the severely disordered solvent (assumed to be EtOH) in the channel. An analysis using the *PLATON SQUEEZE* software<sup>23</sup> indicated the presence of 132 electrons per unit cell (or 33 per formula unit) in these channels. The model reported here for **4S** is based on a solvent-corrected dataset obtained from this procedure.

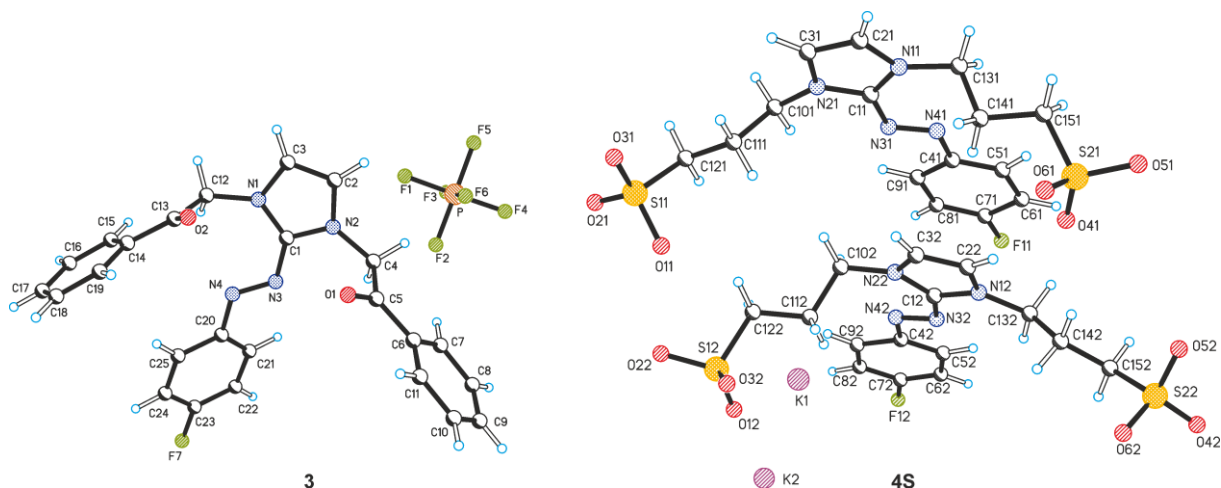


**Figure 4.** Molecular structures of **3** and **4S**

The crystal structure of **5** (Figure 3) has the space group symmetry  $C2/m$ , and its asymmetric unit contains just one half of a formula unit, despite the cation not possessing any symmetry element itself. Instead, the mirror planes in this crystal structure result from the random packing of the cations in two distinct positions which are related by a mirror symmetry operation. Therefore, the complete cation in the structure model is disordered over two alternative, mirror-symmetry related positions. Other possible settings for **5** in lower-symmetry space groups have been tested but were all found to give unsatisfactory results. The diethyl substituents at the imidazolium ring adopt a *cis* arrangement, and the FPDI fragment is nearly planar. The centre of the  $\text{BF}_6$  anion is located on a crystallographic two-fold axis, and one of two independent F atoms is disordered over two positions of equal occupancy (F3/F3A).

The crystal structure of **6** contains two independent formula units (Figure 5). Each of the two independent FPDI units deviates somewhat from planarity, with a maximum angle of  $9.4^\circ$  between the ring mean planes. In one of the hexafluorophosphate ions, the complete set of F atoms is disordered over two positions with an occupancy ratio of 66:34.

Compound **7** forms a hemihydrate ( $\mathbf{7} \cdot 0.5 \text{H}_2\text{O}$ ) whose asymmetric unit contains two formula units of **7** as well as one water molecule (Figure 5). One of the four independent FPDI units deviates significantly from planarity so that its two ring mean planes form an angle of  $21.8^\circ$  with one another. The two independent molecules of **7** are linked by two  $\text{O-H}\cdots\text{N}$  bonds involving their respective OH group and an imidazole N atom. The water molecule (*w*) is H-bonded to the OH group of the first molecule of **7**,  $(w)\text{O-H}\cdots\text{O14}(x+1, y-1, z)$ . It is also bonded to an imidazole ring of the other independent molecule of **7**,  $(w)\text{O-H}\cdots\text{N13}$ , so that the water molecule acts as an H-bonded bridge between two dimers. The resulting infinite H-bonded chain structure (Figure 6) propagates along the  $[1-10]$  direction.



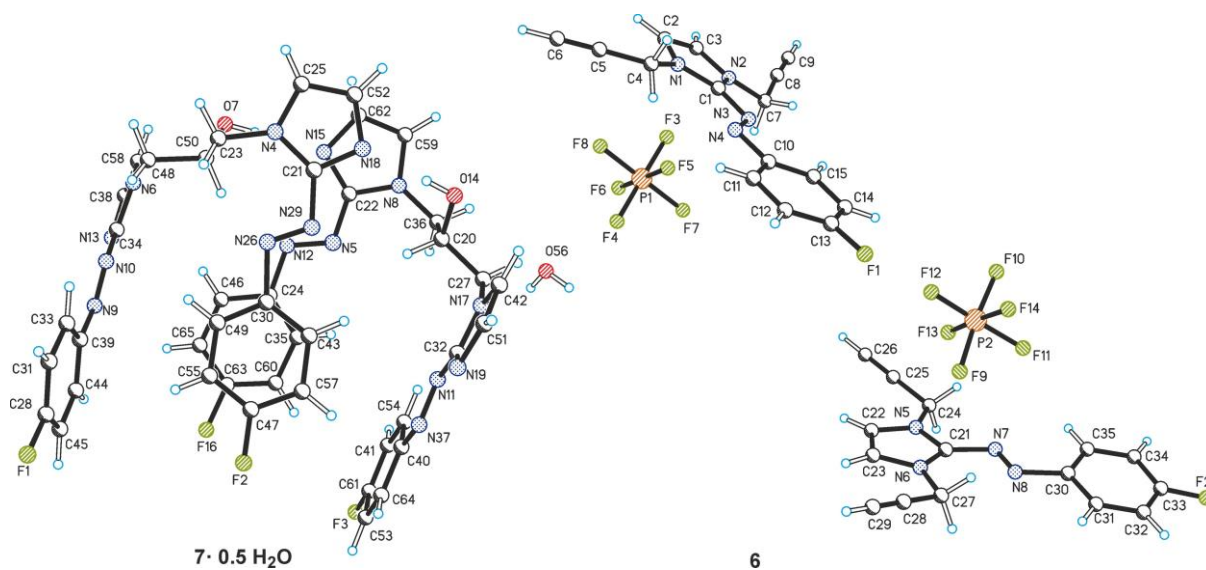


**Figure 5.** Molecular structures of  $7 \cdot 0.5 \text{H}_2\text{O}$  and **6**

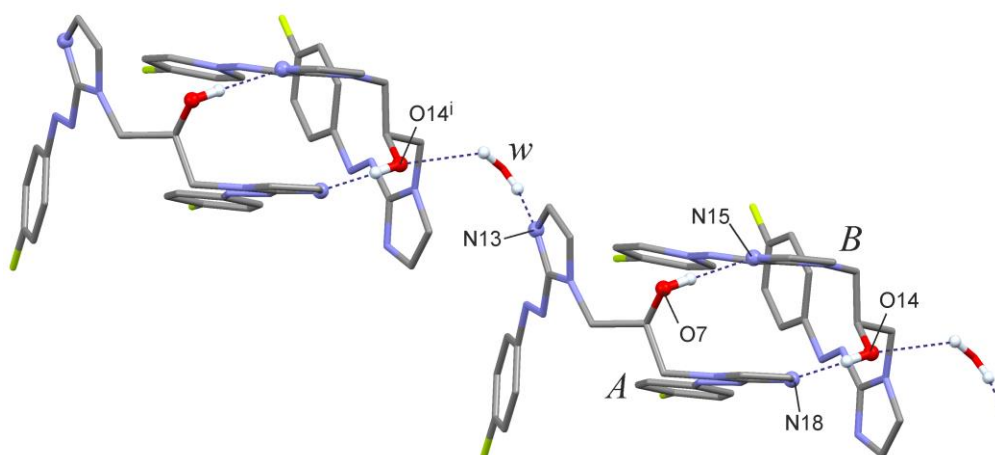


**Figure 6.** H-Bonded chain in  $7 \cdot 0.5 \text{H}_2\text{O}$ , composed of two-point O–H $\cdots$ N-connected dimers of **7** (independent molecules *A* and *B*) and bridging water molecules (*w*; symmetry operation *i*:  $x + 1, y - 1, z$ )

**Table 1.** Crystal data and structure refinement

Compound	<b>1</b>	<b>2 · 0.5 4-VBnCl</b>	<b>3</b>
Moiety formula	C <sub>23</sub> H <sub>20</sub> FN <sub>4</sub> <sup>+</sup> Br <sup>-</sup>	C <sub>27</sub> H <sub>24</sub> FN <sub>4</sub> <sup>+</sup> PF <sub>6</sub> <sup>-</sup> · 0.5(C <sub>9</sub> ClH <sub>9</sub> )	C <sub>25</sub> H <sub>20</sub> FN <sub>4</sub> O <sub>2</sub> <sup>+</sup> PF <sub>6</sub> <sup>-</sup>
Empirical formula	C <sub>23</sub> H <sub>20</sub> BrFN <sub>4</sub>	C <sub>31.50</sub> H <sub>28.50</sub> Cl <sub>0.50</sub> F <sub>7</sub> N <sub>4</sub> P	C <sub>25</sub> H <sub>20</sub> F <sub>7</sub> N <sub>4</sub> O <sub>2</sub> P
Formula weight	451.34	644.78	296.96
Temperature (K)	193	173	193
Wavelength (Å)	0.71073	0.71073	0.71073
Crystal system	Triclinic	Triclinic	Triclinic
Space group	<i>P</i> $\bar{1}$	<i>P</i> $\bar{1}$	<i>P</i> $\bar{1}$
<i>a</i> (Å)	10.0326(8)	11.2452(6)	5.5596(6)
<i>b</i> (Å)	10.0645(9)	11.2953(6)	15.4044(15)
<i>c</i> (Å)	11.3870(10)	13.7935(8)	15.4096(16)
$\alpha$ (°)	83.909(7)	68.182(2)	70.203(9)
$\beta$ (°)	65.052(8)	74.622(2)	88.477(9)
$\gamma$ (°)	77.350(7)	68.802(2)	87.720(8)
Unit cell volume (Å <sup>3</sup> )	1017.07(15)	1499.05(15)	1240.6(13)
<i>Z</i> / <i>Z'</i>	2 / 1	2 / 1	2 / 1
Reflections collected / <i>R</i> <sub>int</sub>	5768 / 0.0296	39912 / 0.0368	6381 / 0.065
Data / restraints / parameters	3699 / 0 / 262	5318 / 67 / 408	4512 / 313 / 408
Goodness-of-fit on <i>F</i> <sup>2</sup>	1.093	1.030	1.109
<i>R</i> 1 [ <i>I</i> > 2 $\sigma$ ( <i>I</i> )]	0.0456	0.0572	0.0487
<i>wR</i> 2 (all data)	0.1061	0.1545	0.1172
Largest diff. peak and hole (e · Å <sup>-3</sup> )	0.875 and -0.511	0.620 and -0.424	0.357 and -0.253
CCDC no.	2154511	2154512	2154517

<b>4S</b>	<b>5</b>	<b>6</b>	<b>7 · 0.5 H<sub>2</sub>O</b>
C <sub>15</sub> H <sub>18</sub> FN <sub>4</sub> O <sub>6</sub> S <sub>2</sub> <sup>-</sup> K <sup>+</sup> [+ solvent]	C <sub>13</sub> H <sub>16</sub> FN <sub>4</sub> <sup>+</sup> BF <sub>4</sub> <sup>-</sup>	C <sub>15</sub> H <sub>12</sub> FN <sub>4</sub> <sup>+</sup> PF <sub>6</sub> <sup>-</sup>	C <sub>21</sub> H <sub>18</sub> F <sub>2</sub> N <sub>8</sub> O · 0.5 H <sub>2</sub> O
C <sub>15</sub> H <sub>18</sub> FKN <sub>4</sub> O <sub>6</sub> S <sub>2</sub>	C <sub>13</sub> H <sub>16</sub> BF <sub>5</sub> N <sub>4</sub>	C <sub>15</sub> H <sub>12</sub> F <sub>7</sub> N <sub>4</sub> P	C <sub>21</sub> H <sub>19</sub> F <sub>2</sub> N <sub>8</sub> O <sub>1.5</sub>
472.55	334.11	412.26	445.44
193	173	183	193
1.54184	0.71073	0.71073	1.54184
Triclinic	Monoclinic	Monoclinic	Triclinic
<i>P</i> $\bar{1}$	<i>C</i> 2/ <i>m</i>	<i>P</i> 2 <sub>1</sub> / <i>c</i>	<i>P</i> $\bar{1}$
11.0710(11)	12.5799(9)	15.1100(6)	12.4041(16)
13.4144(13)	17.2548(13)	14.2857(5)	13.8806(17)
16.8773(16)	7.8174(6)	16.2119(6)	14.1790(16)
90.460(8)	90	90	71.269(11)
105.894(8)	114.144(2)	90.8954(13)	87.089(10)
99.368(8)	90	90	66.619(12)
2374.8(4)	1548.4(2)	3499.0(2)	2113.9(5)
4 / 2	4 / 0.5	8 / 2	4 / 2
10784 / 0.0765	15899 / 0.0417	46694 / 0.0357	26121 / 0.1279
6717 / 0 / 523	1417 / 9 / 181	6141 / 0 / 541	7578 / 0 / 594
0.970	1.008	1.039	1.043
0.0884	0.0571	0.0520	0.0791
0.2618	0.1681	0.1311	0.2605
0.641 and -0.682	0.469 and -0.353	1.461 and -0.641	0.846 and -0.311
2154516	2154515	2154513	2154514

## CONCLUSIONS AND OUTLOOK

Feature-rich covalent stains,<sup>24</sup> belong to the hot topics of contemporary materials chemistry with still growing fields of application. For example, they are highly relevant for microscopy, in particular super-resolution and cleared tissue fluorescence microscopy.<sup>24</sup> Therefore, it seems very inviting, to evaluate suitable fluorophoric 4-fluorophenylazoimidazolium salts as orthogonal biochemical labelling agents. When coming back to the realm of S<sub>N</sub>Ar-reactive secondary amines,<sup>4</sup> organic/inorganic hybrids are also worth being considered for forthcoming research, as the hydrolytic stability of coated siliceous surfaces can be substantially improved by modification with dipodal silanes.<sup>25</sup> Amine-difunctional types, such as bis(trimethoxysilylpropyl)amine, are forming reactive graftings,<sup>26</sup> also capable of anchoring 4-fluorophenylazoimidazolium salts to form (colored) ion exchange resins or monoliths, even with the surplus possibility of on-surface-polymerization. In this regard, the dimer azo-chromophore **7** would, after complete quarternization, as a prophetic example, turn into a doubly dipodal surface primer, which again invites microscopy as a valuable methodology: hot stage chemical coating experiments of microscope slide and cover glass would be directly observable.

## EXPERIMENTAL

Commercially available reagents and solvents (*e.g.* purchased from Merck/Sigma-Aldrich) were used as received unless otherwise stated.

[(*E*)-2-(4-Fluorophenyl)diazenyl]-1*H*-imidazole, [210180-24-0], was prepared following a disclosed procedure.<sup>12</sup> However, this synthesis yields a neutral product, and not a hydrochloride salt, erroneously depicted in this patent literature. In favor of easy workup avoiding chromatography,<sup>15</sup> no emphasis was laid on the optimization of the synthetic procedures with respect to yields. NMR spectra were recorded on a Bruker Avance DPX 300 MHz or a Bruker Avance 4 Neo 700 MHz spectrometer. The 700 MHz NMR spectrometer is equipped with a N<sub>2</sub> cooled Prodigy TCI probe. Standard Bruker pulse programs were used (<sup>1</sup>H: *zg30*; COSY: *cosygpmfqf*; <sup>1</sup>H-<sup>13</sup>C-HSQC: *hsqcedetgpsisp2.2*; <sup>1</sup>H-<sup>13</sup>C-HMBC: *hmbcetgpl3nd*; <sup>13</sup>C: *zgpg30*). In addition, a 1D <sup>19</sup>F spectrum and a <sup>19</sup>F-<sup>13</sup>C HSQC correlation spectrum were acquired on the Bruker Avance 4 Neo 700 MHz spectrometer. High resolution mass spectrometric data were measured on a Thermo Finnigan Q Exactive Orbitrap spectrometer. IR spectra were obtained with a Bruker ALPHA Platinum FT-ATR instrument. UV/VIS reflection spectra were recorded with an Agilent Cary 5000 UV-Vis-NIR Spectrophotometer. For this purpose, the powder was placed into a sample holder. Spectra were recorded in the range of 200 to 700 nm before and after irradiation ( $\lambda = 365$  nm or  $\lambda = 535$  nm, 5 min). For the illumination of the sample, a Prizmatix PRI FC5-LED-WL (five high power Fiberglas coupled LEDs output with potentiometer for manual power control) was used. Melting points were determined on a Kofler Microscope and corrected against reference substances. The instrumentation of

hot stage microscopy (HSM) and Thermogravimetric Analysis (TGA) is described in detail in a preceding communication.<sup>22</sup>

Diffraction intensity data for the single crystal structure determinations of **1**, **3**, **4S** and **7 · 0.5 H<sub>2</sub>O** were recorded with a Oxford Diffraction Xcalibur Ruby Gemini diffractometer and those for **2 · 0.5 4-VBnCl**, **5** and **7** were recorded with a Bruker D8 Quest Photon 100 diffractometer, using MoK $\alpha$  radiation ( $\lambda = 0.7107 \text{ \AA}$ ) or in the case of **4S** and **7** CuK $\alpha$  radiation ( $\lambda = 1.54184 \text{ \AA}$ ). The crystal structures were solved by Direct Methods with *SHELXT*<sup>27</sup> or *SIR 2002*<sup>28</sup> and refined by full-matrix least-squares techniques using *SHELXL*<sup>29</sup>. The solvent molecules in the channel structure of **4S** were found to be severely disordered over multiple orientations, and the structure refinement did not result in a geometrically sensible model of the disordered solvent molecule. Therefore, a *PLATON SQUEEZE* procedure was applied on the data before the final refinement was carried out.<sup>23</sup> CCDC 2154511–7 contain the supplementary crystallographic data for this paper. These data can be obtained free of charge from the Cambridge Crystallographic Data Centre *via* [www.ccdc.cam.ac.uk/structures](http://www.ccdc.cam.ac.uk/structures).

### **1,3-Dibenzyl-2-((4-fluorophenyl)diazenyl)-1H-imidazolium bromide (1)**

2-((4-Fluorophenyl)diazenyl)-1H-imidazole (1 eq.) was suspended in MeCN (3.2 mL per mmol) under argon and cooled in an ice bath. The suspension was treated with potassium ethanolate (1.2 eq.) and the cooling bath was subsequently removed. Next, benzyl bromide was added in excess (10 eq.) and the reaction mixture was stored for one month at room temperature. The suspension was diluted with DMF and MeOH to effect complete dissolution. The crude product was precipitated by the addition of Et<sub>2</sub>O and removed from the mixture by filtration. The product was obtained as dark red crystals after recrystallization from MeOH in 11% yield. Single crystals for X-ray crystallography were grown through slow evaporation of a methanolic solution of compound **1**. <sup>1</sup>H NMR (300 MHz, DMSO-*d*<sub>6</sub>)  $\delta$  8.13 (m, 2H), 7.54 (m, 2H), 7.39 (m, 12H), 5.80 (s, 4H) ppm.

### **2-((4-Fluorophenyl)diazenyl)-1,3-bis-(4-vinylbenzyl)-1H-imidazolium hexafluorophosphate (2)**

2-((4-Fluorophenyl)diazenyl)-1H-imidazole (1 eq.) was suspended in MeCN (3.2 mL per mmol) under argon and cooled in an ice bath. The suspension was treated with potassium ethanolate (1.2 eq.) and the cooling bath was removed. Next, 4-vinylbenzyl chloride was added in excess (10 eq.) and the reaction mixture was let stand at room temperature for several days. Subsequently, just enough MeOH was added to solubilize the suspension, then water was added. The resulting emulsion was washed twice with CH<sub>2</sub>Cl<sub>2</sub>. The aqueous layer was treated with an ammonium hexafluorophosphate solution and then extracted with CH<sub>2</sub>Cl<sub>2</sub>. Evaporation of the solvents gave compound **2** in 46% yield. Crystals of compound **2** that were of sufficient quality for X-ray structure determination were grown from a saturated CH<sub>2</sub>Cl<sub>2</sub>

solution, Mp 169 °C.  $^1\text{H}$  NMR (300 MHz, DMSO- $d_6$ )  $\delta$  7.96 (m, 2H), 7.49 (m, 10H), 7.24 (m, 4H), 6.78 - 6.62 (m, 2H), 5.88- 5.75 (m, 2H), 5.30 - 5.15 (m, 2H), 4.75 (s, 2H). ppm.

**2-((4-Fluorophenyl)diazenyl)-1,3-bis(2-oxo-2-phenylethyl)-1H-imidazolium hexafluorophosphate (3)**

Under argon, an ice cold suspension of 2-((4-fluorophenyl)diazenyl)-1H-imidazole (3.00 g, 15.8 mmol) in MeCN (50 mL) was treated with potassium ethanolate (1.60 g, 19.0 mmol). The color changed from yellow to orange. The ice-bath was removed and stirring continued for 20 min at room temperature. Next, 2-bromoacetophenone (8.00 g, 40.2 mmol) was added. The color changed back to yellow. The suspension was held at reflux temperature for 2 h, diluted with MeCN (50 mL) and stirred at room temperature overnight. The mixture was diluted with Et<sub>2</sub>O (200 mL) to precipitate inorganic salts, which were removed by filtration. The filtrates were concentrated, diluted with CH<sub>2</sub>Cl<sub>2</sub> and treated with aqueous NH<sub>4</sub>PF<sub>6</sub>, to precipitate 150 mg (1.60%) of compound **3** as hexafluorophosphate salt. Single crystals for X-ray crystallography were obtained through slow evaporation of a methanolic solution of compound **3**, Mp 175 °C.  $^1\text{H}$  NMR (300 MHz, DMSO- $d_6$ )  $\delta$  8.15 (s, 2H), 8.13 (s, 2H), 8.11 (s, 2H), 7.83 (t, J = 7.4 Hz, 2H), 7.69 – 7.63 (m, 6H), 7.39 (t, J = 8.8 Hz, 2H), 6.46 (s, 4H) ppm; IR (neat):  $\nu$  3179 (w), 3069 (w), 3013 (w), 2963 (w), 1692 (m), 1596 (m), 1465 (m), 1354 (m), 1306 (w), 1235 (m), 1141 (m), 1078 (w), 1002 (w), 825 (s), 754 (m), 686 (m) cm<sup>-1</sup>.

**3,3'-(2-((4-Fluorophenyl)diazenyl)-1H-imidazolium-1,3-diyl)bis(propane-1-sulfonate) potassium salt (4)**

2-((4-Fluorophenyl)diazenyl)-1H-imidazole (1.00 g, 5.26 mmol) was dissolved in MeOH and potassium ethanolate (0.60 g, 7.10 mmol) was added. A clear orange solution resulted. Propane-1,3-sultone (1.50 mL, 2.10 g, 17 mmol) was added and the mixture stirred at room temperature. After two days, a second portion of propane-1,3-sultone (1.00 mL, 1.40 g, 11 mmol) was added. After stirring overnight, one half of the reaction mixture was refluxed for 1 h. The other half was mixed with Et<sub>2</sub>O to precipitate the product, which was isolated by filtration and washed with Et<sub>2</sub>O. The first half was worked up analogously. The crude products were each recrystallized from EtOH to yield 207 mg (8%) of yellow solids with very high solubility in water, Mp 260 °C (dec.).  $^1\text{H}$  NMR (300 MHz, DMSO- $d_6$ )  $\delta$  8.37 (s, 2H), 8.11 (s, 2H), 7.54 (s, 2H), 4.62 (s, 4H), 3.46 (s, 4H), 2.15 (s, 4H) ppm; IR (neat):  $\nu$  3437 (w), 3103 (w), 2977 (w), 2630 (w), 2539 (w) 1590 (m), 1460 (m), 1309 (w), 1172 (s), 1034 (s), 856 (m), 802 (w), 733 (w) cm<sup>-1</sup>.

**(1,3-Diethyl-2-((4-fluorophenyl)diazenyl)-1H-imidazolium tetrafluoroborate (5)**

Triethyloxonium tetrafluoroborate (8.78 g, 46.2 mmol) was dissolved in CH<sub>2</sub>Cl<sub>2</sub> (110 mL) and cooled in an ice-water bath, before 2-((4-fluorophenyl)diazenyl)-1H-imidazole (4.00 g, 21.0 mmol) was added. The transiently formed suspension cleared up in several minutes and an orange solution formed. The reaction mixture was stirred at room temperature overnight. Next, solid Na<sub>2</sub>CO<sub>3</sub> (1.76 g, 21.0 mmol) was added, and the suspension was treated with H<sub>2</sub>O (100 mL) to effect partial precipitation of the product (1.70 g, 24%). The filtrate was diluted with Et<sub>2</sub>O (300 mL) to yield a second crop (1.30 g, 19%). Single crystals for crystal structure determination were obtained through slow evaporation of a CH<sub>2</sub>Cl<sub>2</sub> solution of compound **5** as an orange solid, melts sluggish between 200 and 220 °C. <sup>1</sup>H NMR (300 MHz, DMSO-*d*<sub>6</sub>) δ 8.15 (m, 4H), 7.56 (m, 2H), 4.54 (m, 4H), 1.47 (s, 6H) ppm; <sup>13</sup>C NMR (176 MHz, CH<sub>2</sub>Cl<sub>2</sub>-*d*<sub>2</sub>) δ 168.63, 168.54, 167.15, 167.06, 149.77, 149.17, 146.71, 142.92, 128.21, 128.15, 127.46, 127.40, 124.12, 123.28, 121.34, 121.17, 117.82, 117.69, 117.55, 117.37, 46.26, 43.96, 16.06, 15.69 ppm (equilibrium of isomers); <sup>19</sup>F NMR (659 MHz, CH<sub>2</sub>Cl<sub>2</sub>-*d*<sub>2</sub>) δ -100.33, -151.86 ppm; IR (neat): ν 3590 (w), 3144 (w), 2994 (w), 1589 (m), 1524 (m), 1482 (m), 1292 (w), 1229 (m), 1145 (m), 1032 (s), 856 (m), 780 (m), 703(m) cm<sup>-1</sup>; HRMS (ESI<sup>+</sup>) M<sup>+</sup> for C<sub>13</sub>H<sub>16</sub>FN<sub>4</sub><sup>+</sup> calcd.: 247.1345, found: 247.1355; HRMS (ESI<sup>-</sup>): M<sup>-</sup> for BF<sub>4</sub><sup>-</sup> calcd.: 87.0035, found: 87.0021.

**2-((4-Fluorophenyl)diazenyl)- 1,3-bis-(propargyl)-1H-imidazolium hexafluorophosphate (6)**

2-((4-Fluorophenyl)diazenyl)-1H-imidazole (1.00 g, 5.26 mmol) was treated with propargyl benzenesulfonate (2.27 g, 11.6 mmol) at room temperature overnight. Subsequently, CaCO<sub>3</sub> (526 mg, 5.26 mmol) was added and stirring was continued for 24 h. The orange suspension was diluted with MeOH, filtered and the filtrates were diluted with Et<sub>2</sub>O to precipitate 2.68 g (126%) of the crude product that contained residual calcium salts. Single crystals were obtained after treating the product with ammonium hexafluorophosphate (1 eq.) and slow evaporation from MeOH, Mp 176 °C (dec., onset of decomposition 137 °C). <sup>1</sup>H NMR (300 MHz, DMSO-*d*<sub>6</sub>) δ 8.21 (s, 2H), 7.59 (m, 2H), 7.30 (m, 2H), 5.49 (m, 4H), 3.80 (m, 2H) ppm.

**1,3-Bis(2-((4-fluorophenyl)diazenyl)-1H-imidazol-1-yl)propan-2-ol (7)**

Under argon, 2-((4-fluorophenyl)diazenyl)-1H-imidazole (2.00 g, 10.5 mmol) in dry MeOH (60 mL) was treated with potassium ethanolate (974 mg, 11.6 mmol) at room temperature for 30 min. Subsequently, epichlorohydrin (0.53 mL, 6.7 mmol) was added dropwise and the reaction was stirred at room temperature overnight. A yellow precipitate was isolated by filtration and washed with water and Et<sub>2</sub>O to obtain 0.80 g (17%) of compound **7**, Mp 204 - 207 °C. <sup>1</sup>H NMR (300 MHz, DMSO-*d*<sub>6</sub>) δ 8.02 – 7.08 (m, 12H), 5.75 (s, 1H), 4.73 – 4.09 (m, 5H) ppm; IR (neat): ν 3537 (w), 3359 (w), 3261 (w), 3103 (w), 2938

(w), 2864 (w), 2780 (w), 2556 (w), 2449 (w), 2343 (w), 1715 (w), 1590 (m), 1498 (m), 1362 (m), 1291 (m), 1226 (s), 1130 (w), 1092 (m), 1036 (w), 655 (w), 845 (s), 778 (m)  $\text{cm}^{-1}$ .

## ACKNOWLEDGEMENTS

The authors are grateful to Patrick Ladurner and Marcus Rauter for technical assistance.

## REFERENCES

1. H. Pauly, *Z. Physiol. Chem.*, 1904, **42**, 508.
2. R. G. Farga and F. L. Pyman, *J. Chem. Soc., Trans.*, 1919, **115**, 217.
3. L. M. Anderson, A. R. Butler, C. Glidewell, D. Hart, and N. Isaacs, *J. Chem. Soc., Perkin Trans. II*, 1989, 2055.
4. H. Baumann and J. Dehnert, *Chimia*, 1961, **15**, 163.
5. S. S. Jiang, J. H. Qiu, and C. M. Jin, *J. Chem. Res.*, 2014, **38**, 414.
6. A. Nandi, C. Sen, D. Mallick, R. K. Sinha, and C. Sinha, *Adv. Mater. Phys. Chem.*, 2013, **3**, 133.
7. T. K. Misra, D. Das, C. Sinha, P. Gosh, and C. K. Pal, *Inorg. Chem.*, 1998, **37**, 1672.
8. D. Das, B. G. Chand, J. S. Wu, T.-H. Lu, and C. Sinha, *J. Mol. Struct.*, 2007, **842**, 17.
9. C. Schütt, G. Heitmann, T. Wendler, B. Krahwinkel, and R. Herges, *J. Org. Chem.*, 2016, **81**, 1206.
10. S. Rohrbach, A. J. Smith, J. H. Pang, D. L. Poole, T. Tuttle, S. Chiba, and J. A. Murphy, *Angew. Chem. Int. Ed.*, 2019, **58**, 16368.
11. F. Bachmann, C. Cremer, B. Froehling, B. P. Murphy, G. Zhang, and P. M. Torgerson, WO2016146813, 2016.
12. V. P. Eliu, B. Froehling, and D. Kauffmann, [WO2007025889](#), 2007.
13. C. Blaise and V. Bruckbuchler, [WO2017081314](#).
14. H. P. Kühltau, DE2908135, 1980.
15. C. Lin, L. Yang, M. Xu, Q. An, Z. Xiang, and X. Liu, *RSC Adv.*, 2016, **6**, 51552.
16. M. Lampl, G. Laus, K. Wurst, H. Huppertz, and H. Schottenberger, *IUCrData*, 2017, **2**, 171207.
17. H. W. Wanzlick and H. J. Kleiner, *Angew. Chem.*, 1963, **75**, 1204.
18. S. Yamada, [US20070015912](#), 2007.
19. C. Cremer, O. Wallquist, V. P. Eliu, and K. R. Nivalkar, [US7794509](#), 2010.
20. K-P. Zhang, T.-Q. Jin, J.-Q. Zhou, T.-T. Ma, and C.-M. Jin, *J. Heterocycl. Chem.*, 2017, **54**, 3065.
21. L. S. Dahne, G. Egri, M. Hecht, M. K. Herrlein, M. Klickermann, B. P. Murphy, M. J. Patten, T. Schafer, S. R. Schofield, C. Uzum, and I. R. Weber, WO2017189539A1, 2017.

22. L. Fliri, T. Gelbrich, U. J. Griesser, G. Partl, F. R. S. Purtscher, S. Neuner, K. Erharter, K. Wurst, V. Kahlenberg, D. E. Braun, T. S. Hofer, A. Rössler, and H. Schottenberger, [\*Z. Anorg. Allg. Chem.\*, 2021, \*\*647\*\*, 365.](#)
23. A. Spek, [\*Acta Cryst.\*, 2015, \*\*C71\*\*, 9.](#)
24. C. Mao, M. Y. Lee, J. R. Jhan, A. R. Halpern, M. A. Woodworth, A. K. Glaser, T. J. Chozinski, L. Shin, J. W. Pippin, S. J. Shankland, J. T. C. Liu, and J. C. Vaughan, [\*Sci. Adv.\*, 2020, \*\*6\*\*, eaba4542.](#)
25. J. J. DeLuca and G. D. Tucker, [\*US 20120145037A1\*, 2012.](#)
26. B. Arkles, Y. Pan, G. L. Larson, and M. Singh, [\*Chem. Eur. J.\*, 2014, \*\*20\*\*, 9442.](#)
27. G. Sheldrick, [\*Acta Cryst.\*, 2015, \*\*A71\*\*, 3.](#)
28. M. C. Burla, M. Camalli, B. Carrozzini, G. L. Cascarano, C. Giacovazzo, G. Polidori, and R. Spagna. [\*J. Appl. Cryst.\*, 2003, \*\*36\*\*, 1103.](#)
29. G. Sheldrick, [\*Acta Cryst.\*, 2015, \*\*C71\*\*, 3.](#)